Compositeness, Feynman Diagrams, and the Reggeized Absorption Model*

CLIFFORD RISK
Lawrence Radiation Laboratory, University of California, Berkeley, California 94720
(Received 26 June 1970)

In this paper we derive the Reggeized absorption model from field-theoretic diagrams. This model has been used to describe a large number of quasi-two-body reactions. It involves a Regge-cut correction to Regge-pole amplitude which is generated by the exchange of the Regge pole and a Pomeranchuk pole. The cut features the product of the Reggeon and Pomeranchon (without complex conjugation of either) and a large magnitude for the cut (coherent inelastic effects add to the original cut term). The fundamental physical assumption of our derivation is that physical particles are composite objects of constituent pieces of matter. In a scattering process, some of the constituent matter takes part in the scattering while the rest stands by as a spectator. These ideas lead us to describe double-scattering processes by a class of diagrams involving exchange of two Reggeons in the crossed channel and propagation of composite physical particles in the direct channel. When the direct-channel particles are Reggeized, we obtain an expression for the Regge box diagram. We begin our analysis of diagrams by discussing the Amati-Fubini-Stanghellini diagram and similar diagrams to demonstrate how the absence of third double-spectral functions leads to the absence of a cut. For simple diagrams, we find that we are forced to invoke properties of form factors to show absence of the cut, but that for sufficiently composite diagrams the absence of the cut rests solely on the absence of the third double-spectral functions. Next we discuss the Mandelstam diagram and similar diagrams to demonstrate how the presence of third double-spectral functions leads to cuts. For each diagram we bring the expression for the amplitude to the form of the absorption model. Finally, we study the general class of diagrams referred to above. These diagrams feature compositeness in the direct channel (physical particles are composite), third double-spectral functions (physical particles have definite signature; no exchange degeneracy), and two-Reggeon exchange (double scattering and the Glauber spectator approximation). By assuming saturation of direct-channel amplitudes by physical states, we are led to an absorption formula (no complex conjugations) that includes the coherent inelastic factor λ (diffraction production of direct-channel resonances).

I. INTRODUCTION

THE idea that the asymptotic behavior of a scattering amplitude $A(s,t)$ is determined by singularities of the partial-wave amplitude $f_j(t)$ in the complex j plane is ten years old.[1] During this decade, this idea has been studied both phenomenologically, with various models that describe specific reactions,[2] and theoretically, with the investigation of sums of Feynman diagrams that define amplitudes with various types of j-plane singularities.[3,4]

The main school of thought has been that $f_j(t)$ is meromorphic in the j plane with simple poles at values $j=\alpha_i(t)$ that correspond to physical particles. Phenomenological models with these Regge poles were used to fit a large number of elastic and quasi-two-body reactions. Meanwhile, the theoretical study of various field theories led to the conclusion that Regge poles arise in field theories also.

However, the use of phenomenological models with poles alone led to several difficulties and complications in the attempt to explain features of differential cross sections[5]—such as dips, crossovers, and forward peaks (in π-exchange reactions)—and features of total cross sections—such as the rise at Serpukhov energies. This suggested that in the j plane the properties of $f_j(t)$ might be more involved that containing poles only. Meanwhile, the study of field-theory models produced amplitudes with fixed poles, moving cuts, fixed cuts, and essential singularities.[3]

One of the earlier models with more complicated singularities was developed by Abers *et al.*[6] (following earlier work by Udgaonkar and Gell-Mann[7]) in the study of π-deuteron scattering. Glauber[8] had shown that the amplitude $A_{\pi d}$ could be expressed as a sum of single and double πN scatterings. Abers *et al.* then showed that these scatterings correspond to the amplitudes for the diagrams of Fig. 1 where the particles in the direct channel (cut by the dashed line) are to be evaluated near the mass shell. Furthermore, if the

* Preliminary versions of the present work have appeared in Proceedings of the Regge Cut Conference, University of Wisconsin, 1969 (unpublished), and LRL Report No. UCRL-19453, 1970 (unpublished). The Sudakov variable techniques, used extensively here, were first applied to diagrams with Reggeons in a comprehensive work to develop a Reggeon calculus by V. N. Gribov (Ref. 19). In the work at hand we have employed these techniques to analyze the diagrams considered here in obtaining the absorption model. After our work was completed, our attention was called to a series of six papers by Gribov and Migdal, Kaidalov and Karnakov, and ter-Martirosyan which extended the earlier work of Gribov and, among other things, obtained the absorption model. In Sec. IV we compare our approach with theirs and discuss the similarities and differences.

[1] T. Regge, Nuovo Cimento **14**, 951 (1959).

[2] G. E. Hite, Rev. Mod. Phys. **41**, 669 (1969).

[3] R. J. Eden, P. V. Landshoff, D. I. Olive, and J. C. Polkinghorne, *The Analytic S-Matrix* (Cambridge U. P., Cambridge, England, 1966).

[4] R. J. Eden, *High Energy Collisions of Elementary Particles* (Cambridge U. P., Cambridge, England, 1967).

[5] F. Henyey, G. L. Kane, J. Pumplin, and M. Ross, Phys. Rev. **182**, 1579 (1969), hereafter referred to as HKPR.

[6] E. S. Abers, H. Burkhardt, V. L. Teplitz, and C. Wilkin, Nuovo Cimento **42**, 365 (1965).

[7] B. M. Udgaonkar and M. Gell-Mann, Phys. Rev. Letters **8**, 346 (1962).

[8] R. J. Glauber, in *Lectures in Theoretical Physics*, edited by W. E. Brittin and L. G. Dunham (Interscience, New York, 1959), Vol. I; V. Franco and R. J. Glauber, Phys. Rev. **142**, 1195 (1966).

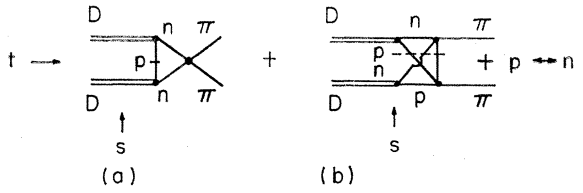

FIG. 1. Diagrams for πd scattering.

single-scattering terms were given by Regge poles

$$A_{\pi p}(s,t)=\beta(t)s^{\alpha(t)}, \tag{1}$$

then the double-scattering term of Eq. (1) took the form of an amplitude with a cut in the j plane at $j(t)=2\alpha(\frac{1}{4}t)-1$,

$$A(\text{double})=s^{j(t)}/\ln s. \tag{2}$$

This cut term, the Glauber shadow correction, was observed experimentally in differential and total cross sections. However, it was next shown that if in Fig. 1(b) the contribution was evaluated from the region of integration where the π was off the mass shell, this exactly canceled the cut. The sum of both contributions behaved as $(\ln s)/s^3$ and had no leading cut.[9]

This type of theoretical difficulty also occurs in models that describe two-body processes in terms of a multiple scattering series. In describing $\pi^- p\to\pi^0 n$, one is led to the formula[5] (where $A_{\text{el}}\sim -i$)

$$A(s,t)=A_\rho(s,t)-\frac{i}{32\pi^2}\int d\Omega\, A_\rho(s,t_1)A_{\text{el}}(s,t_2), \tag{3}$$

where A_ρ is the amplitude for ρ exchange, and A_{el} is the elastic π-nucleon amplitude. This can be derived from either a Glauber eikonal series[10,11] or from the Sopkovitch formula.[5] It can also be derived from Feynman diagrams of the type of Fig. 2(b). The second term in Eq. (3) corresponds to the contribution from Fig. 2(b) in which the direct channel π^0, n are evaluated on the mass shell. However, if one evaluates the contribution from the region where the π^0,n go off the mass shell, the previous term is again exactly canceled and their sum has no cut.

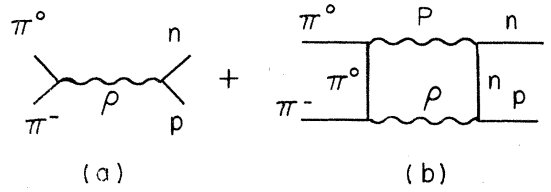

FIG. 2. Diagrams for absorption model.

FIG. 3. AFS diagram.

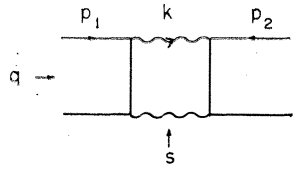

The difficulty encountered in both of these examples is related to the diagram version of the work of AFS.[12] The discontinuity of the amplitude of Fig. 3 across the branch cut of the two-particle direct-channel state is given by[12]

$$\text{Im}A(s,t)\propto\int\frac{d^2k}{s}A_1(s,t_1)A_2^*(s,t_2), \tag{4}$$

and $A(s,t)$ has a branch point at $j(t)=2\alpha(\frac{1}{4}t)-1$. However, in a ladder representation of a Reggeon,[13] there are further contributions to the unitarity equation that cancel the cut.[14]

Although the three diagrams considered do not have cuts, there are diagrams which do have cuts, for example, the double crossed diagram[3,15] of Fig. 4.

In this work we will reconcile these results for Feynman diagrams on the one hand with the experimentally valid multiple-scattering models on the other. To do this, we start from assumptions about the composite structure of physical particles, and combine them with the ideas of multiple scattering. This leads us to a class of Feynman diagrams which can be evaluated in the high-energy limit. The final expression we are led to agrees with the multiple-scattering models discussed above.

The organization of the paper is as follows. In Sec. II A we point out the features of the AFS diagram that cause it not to have a cut. In Sec. II B we discuss why the double crossed diagram of Fig. 4 does have a cut, and we bring the amplitude to a form similar to the absorption model. Next we extend the results to more complicated diagrams with cuts. In Sec. II C we discuss two further diagrams without cuts, drawing out the role that third double-spectral functions and form

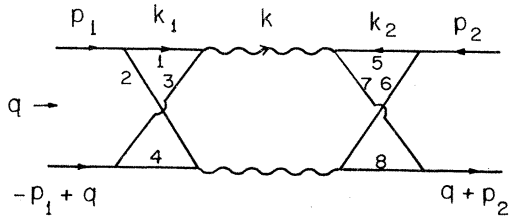

FIG. 4. Mandelstam diagram.

[9] A solution to this difficulty, different from the one we present, has been suggested by Dr. C. Wilkin, University College, London, report (unpublished).

[10] R. C. Arnold, Phys. Rev. **153**, 1523 (1967); ANL Report No. ANL/HEP 6804, 1968 (unpublished).

[11] C. B. Chiu and J. Finkelstein, Nuovo Cimento **57A**, 649 (1968).

[12] D. Amati, S. Fubini, and A. Stanghellini, Phys. Letters **1**, 29 (1962), referred to as AFS.

[13] P. G. Federbush and M. T. Grisaru, Ann. Phys. (N.Y.) **22**, 263 (1963); **22**, 299 (1963).

[14] J. C. Polkinghorne, Phys. Letters **4**, 24 (1963).

[15] S. Mandelstam, Nuovo Cimento **30**, 1127 (1963); **30**, 1148 (1963).

factors play in the analysis. This leads to the analysis in Sec. II D of a very general class of diagrams in which the presence of a cut is thrown completely onto the presence of third double-spectral functions.

In Sec. III we present our view of the composite structure of physical particles and combine this with the diagram results to obtain the derivation of the absorption model. We compare our results with the work of Gribov *et al.* in Sec. IV. In Sec. V we summarize the assumptions, results, and unsolved problems of the paper.

II. MATHEMATICAL DERIVATIONS

A. AFS Diagram

To begin, we briefly point out the features of Rothe's treatment[16,17] of the AFS diagram that are relevant to our later derivation. In terms of mass variables, the amplitude is given by

$$A(s,t)\propto\frac{1}{s}\int_{\lambda(t,t_1,t_2)\leq 0}\frac{dt_1dt_2}{(-\lambda)^{1/2}}\int_{\lambda(s,s_1,s_2)\geq 0}ds_1ds_2 \times\frac{R(s,t_1;s_1,s_2)R(s,t_2;s_1,s_2)}{(s_1-m^2+i\epsilon)(s_2-m^2+i\epsilon)}, \quad (5)$$

where

$$\lambda(a,b,c)=a^2+b^2+c^2-2ab-2ac-2bc\,.$$

As a function of s_1, the integrand of Eq. (5) has singularities in the lower half-plane consisting of a pole at $s_1=m^2-i\epsilon$ and cuts from the form factors of the Regge amplitudes. Also, it is known[14,18] that as s_1 becomes large,

$$R(s,t;s_1,s_2)\to 1/s\,. \quad (6)$$

(This is valid in the limit s fixed, $s_1\to\infty$, and also in the limit $s\sim s_1\to\infty$.) The s_1 integration runs from $s_1=-\infty$ to $s_1\sim s$ (Fig. 5). Therefore, if we distort the s_1—and similarly s_2—integration in the lower half-plane, we obtain

$$A(s,t)\propto\frac{1}{s}\int\frac{dt_1dt_2}{(-\lambda)^{1/2}}R(s,t_1)R(s,t_2)+A_2(s,t)+A_3(s,t), \quad (7)$$

where $R(s,t_i)$ is the Regge amplitude evaluated on the mass shell, A_2 is the contribution from the cuts in the mass variables, and $A_3(s,t)$ is the contribution from the large semicircles. This last term is negligible because of Eq. (6). The first term in Eq. (7) is the usual AFS amplitude [but without complex conjugation of $R(s,t_2)$].

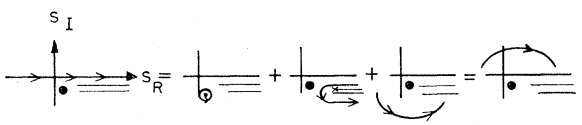

FIG. 5. Integration contour for Fig. 3 in the complex s_1 plane.

On the other hand, if we close the contour of S_i integration in the upper half-plane, we obtain for $A(s,t)$ only a term similar to $A_3(s,t)$, which vanishes as $s\to\infty$. Hence we conclude that $A(s,t)$ must vanish as $s\to\infty$ [the Feynman parameter technique gives $(\ln s)/s^3$], and the apparent cut of the first term in Eq. (7) is canceled by $A_2(s,t)$.

To summarize, the cut does not appear because of (a) the absence of a third double-spectral function, and (b) the presence of form factors. We shall see that the correct interpretation of these two features leads to the Reggeized absorption model.

B. Diagrams with Cuts

We now turn to diagrams that do have cuts, leading to the general diagram of Sec. II D that will connect with our ideas of the composite structure of physical particles and yield the absorption model.

First consider the double crossed diagram of Fig. 4. We follow the treatment by Gribov,[19] and then extend the analysis further to obtain a result resembling the absorption model. The amplitude of Fig. 4 is given by[16,19]

$$A(s,t)=i\int(d^4kd^4k_1d^4k_2/\prod_{i=1}^{8}d_i)R(k_1,k_2,k) R'(p_i-k_1,\,p_2-k_2,\,q-k). \quad (8a)$$

The essential feature of the analysis is to note from Eq. (6) that the internal Regge amplitudes R and R' become small if their external masses d_i become large as fast as or faster than s. Therefore, the dominant contribution to Eq. (8a) comes from the region of integration where d_i remains finite relative to s as s goes to infinity. After s has become asymptotic, the integration over the remaining large values of d_i can be completed. To express this precisely, let Λ be a finite number and define

$$A_\Lambda(s,t)=i\int d^4kd^4k_1d^4k_2RR'\prod_{i=1}^{8}\frac{\Theta(\Lambda-d_i^2)}{d_i}. \quad (8b)$$

Then the above arguments state the leading behavior of $A(s,t)$ is given by

$$\lim_{s\to\infty}A(s,t)=\lim_{\Lambda\to\infty}[\lim_{s\to\infty}A_\Lambda(s,t)]. \quad (8c)$$

[16] H. J. Rothe, Phys. Rev. **159**, 1471 (1967).
[17] C. Wilkin, Nuovo Cimento **31**, 377 (1964).
[18] This is also easily seen from a d-line analysis of the Reggeon in the ladder representation.
[19] V. N. Gribov, in *Proceedings of 1967 International Conference on Particles and Fields*, edited by C. R. Hagen, G. Guralnik, and V. S. Mathur (Interscience, New York, 1967); Zh. Eksperim. i Teor. Fiz. **53**, 654 (1967) [Soviet Phys. JETP **26**, 414 (1968)]. Gribov applied to diagrams with Reggeons the variable techniques of V. V. Sudakov, Zh. Eksperim. i Teor. Fiz. **30**, 87 (1956) [Soviet Phys. JETP **3**, 65 (1956)].

To perform the analysis embedded in Eqs. (8a) and (8c), it is convenient to replace the external momenta p_1, p_2 by lightlike momenta p_1', p_2' defined to order $1/s$ by

$$p_1'=p_1-\frac{m^2}{s}p_2\,,\quad p_2'=p_2-\frac{m^2}{s}p_1\,.$$

The momentum transfer is given by $q=(t/s)(p_2'-p_1')+Q$, where Q is a two-dimensional vector perpendicular to the incident vectors p_1, p_2. The Sudakov variables of integration are introduced by

$$k=\alpha p_2'+\beta p_1'+K\,,\quad k_i=\alpha_i p_2'+\beta_i p_i'+K_i \quad \text{for } i=1,2,$$
$$d^4k=\tfrac{1}{2}|s|\,d\alpha\,d\beta\,dk,\ \text{etc.}\,,$$

where K, K_i are again two-dimensional vectors perpendicular to p_1, p_2. In terms of these variables, the denominators for the left-hand side of Fig. 4 become

$$d_1=k_1^2-m^2+i\epsilon=\alpha_1\beta_1 s+K_1^2-m^2+i\epsilon\,,$$

$$d_2=(p_1-k_1)^2-m^2+i\epsilon=\left(\alpha_1-\frac{m^2}{s}\right)\times(\beta_1-1)s+K_1^2-m^2+i\epsilon\,,$$

$$d_3=(k_1-k)^2-m^2+i\epsilon=(\alpha_1-\alpha)(\beta_1-\beta)s+(K_1-K)^2-m^2+i\epsilon\,, \quad (9)$$

$$d_4=(k_1-k+q-p_1)^2-m^2+i\epsilon=\left(\alpha_1-\alpha+\frac{t}{s}-\frac{m^2}{s}\right)\times\left(\beta_1-\beta-\frac{t}{s}-1\right)s+(K_1-K-Q)^2-m^2+i\epsilon\,,$$

with similar expressions on the right-hand side.

Performing the analysis of Eqs. (8a) and (8b), we first find the region of integration over which $d_i\leq\Lambda$. By solving the equations $d_1,d_2=O(\Lambda)$ for α_1, β_1, we find from Eq. (14) that $\alpha_1=O(\Lambda/s)$, $\beta_1=O(\Lambda)$. After a similar analysis on d_3, d_4; d_5, d_6; d_7, d_8, we conclude that the dominant region of integration as $s\to\infty$ is given by

$$\alpha_1,\alpha,\beta,\beta_2=O(\Lambda/s)\,;\quad \beta_1,\alpha_2=O(\Lambda)\,. \quad (10)$$

Comparing Eq. (10) with Eq. (9), we see that we can neglect β relative to β_1, and α relative to α_2. If we change variables $\alpha_1 s\to\alpha_1$, $\alpha s\to\alpha$, $\beta s\to\beta$, $\beta_2 s\to\beta$, Eqs. (9) become

$$\begin{aligned}
d_1&=\alpha_1\beta_1+K_1^2-m^2+i\epsilon\,,\\
d_2&=(\alpha_1-m^2)(\beta_1-1)+K_1^2-m^2+i\epsilon\,,\\
d_3&=(\alpha_1-\alpha)\beta_1+(K_1-K)^2-m^2+i\epsilon\,,\\
d_4&=(\alpha_1-\alpha+t-m^2)(\beta_1-1)+(K_1-K-Q)^2-m^2+i\epsilon\,,
\end{aligned} \quad (11)$$

and the Regge energies, momentum transfers, and direct-channel energies become

$$\begin{aligned}
&U_1\to\alpha_2\beta_1 s\,,\quad U_2\to(1-\alpha_2)(1-\beta_1)s\,,\\
&k^2=K^2\,,\quad (q-k)^2=(Q-K)^2\,,\\
&s_1=m^2-\alpha+K^2\,,\quad s_2=m^2+\beta+K^2\,.
\end{aligned} \quad (12)$$

The factors α_2, β_1, etc. in Eq. (12) tell what fraction of the original energy s flows through the Reggeons and what portion flows down the sides of the diagram. We see that the terms $d_1,\ \ldots,\ d_4$ depend only on the variables of the left-hand loop—α_1, β_1, K_1—and on α, K, but not on β. Similar dependence is seen for the terms $d_5,\ \ldots,\ d_8$.

Next we assume that the Regge amplitudes of Eq. (8a) can be written in the factorized form

$$R=g_1(d_1,d_3,k^2)e^{-\frac{1}{2}i\pi\phi_1(k^2)}U_1^{\phi_1(k^2)}g_2(d_5,d_7,k^2)\,,$$
$$R'=g_1'(d_2,d_4,(q-k)^2)e^{-\frac{1}{2}i\pi\phi_2[(q-k)^2]}U_2^{\phi_2[(q-k)^2]}\times g_2(d_6,d_8,(q-k)^2)\,.$$

Then Eq. (8a) can be recast into the following form:

$$A_\Lambda(s,t)\propto\int_{O(\Lambda)}dK\,(e^{-i\pi/2}s)^{\phi_1(K^2)+\phi_2[(Q-K)^2]-1}\times N_1(K,Q)N_2(K,Q)\,, \quad (13a)$$

$$N_1(K,Q)=\int_{O(\Lambda)}d\alpha\,(d\alpha_1 d\beta_1 dK_1/\prod_{i=1}^{4}d_i)\times g_1 g_1'\beta_1^{\phi_1}(1-\beta_1)^{\phi_2}\,, \quad (13b)$$

$$N_2(K,Q)=\int_{O(\Lambda)}d\beta\,(d\alpha_2 d\beta_2 dK_2/\prod_{i=5}^{8}d_i)\times g_2 g_2'\alpha_2^{\phi_1}(1-\alpha_2)^{\phi_2}\,. \quad (13c)$$

Here we see that A_Λ is an integral over the usual energy term $s^{\phi_1+\phi_2-1}$, times structure functions N_1 and N_2 that involve the Feynman amplitudes, the form factors, and the Regge energy factors on each side of the diagram.

Now let $\Lambda\to\infty$ in accord with Eq. (8c). We denote the integrand of N_1 by

$$A_1(\alpha,K,Q)=\int_{-\infty}^{+\infty}(d\alpha_1 d\beta_1 dK_1/\prod_{i=1}^{4}d_i)\times g_1 g_1'\beta_1^{\phi_1}(1-\beta_1)^{\phi_2}\,. \quad (14)$$

Note from Eq. (14) that β_1 runs between 0 and +1 only. If $\beta_1<0$, then the integrand as a function of g_1 has singularities that all lie in the upper half-plane [see Eq. (11) and Fig. 6]; the g_1 contour of integration can be closed in the lower half-plane to give zero. If $\beta_1>1$, the singularities all lie in the lower half-plane. But if $0<\beta_1<1$, then the singularities pinch the contour of integration and the integral is nonzero.

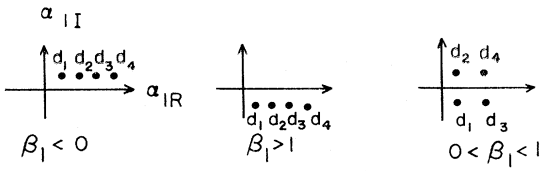

FIG. 6. Singularities of the α integrand in the complex α plane. The integration on α runs from $-\infty$ to $+\infty$.

To bring $A(s,t)$ into the form of the absorption model, we find it necessary to understand the analytic properties of A_1. This can be investigated in the following way. (We neglect the form factors, which can be handled by dispersing in their masses.[20]) Introduce Feynman parameters[20–22] into Eq. (14) via

$$\prod_{j=1}^{4}\frac{1}{d_j}=\left(\frac{1}{i}\right)^4\int_0^\infty\left(\prod_{j=1}^{4}d\lambda_j\right)\exp\left(i\sum_{j=1}^{4}\lambda_j l_j\right). \tag{15}$$

(The $i\epsilon$ in d guarantees convergence.) Then, the dK_1 integration can be done directly. The $d\alpha_1$ integration can be done by using

$$\int_{-\infty}^{+\infty}d\alpha\, e^{i\alpha B}\propto\delta(B). \tag{16a}$$

The quantity B involves β_1, and this allows the $d\beta_1$ integration to be performed. We find

$$\beta_1=\frac{\lambda_2+\lambda_4}{\lambda_1+\lambda_2+\lambda_3+\lambda_4} \tag{16b}$$

and that

$$A_1(s_1,t;l_1,l_2)\propto\int_0^\infty\left(\prod_{i=1}^{4}d\lambda_i\right)\left(\frac{\lambda_2+\lambda_4}{C}\right)^{\phi_1}\times\left(\frac{\lambda_1+\lambda_3}{C}\right)^{\phi_2}\frac{e^{iD(\lambda,s_1,u_1)/C(\lambda)}}{[C(\lambda)]^2}, \tag{17a}$$

where

$$D(\lambda,s_1,u_1)=\lambda_2\lambda_3 s_1+\lambda_1\lambda_4 u_1+\lambda_1\lambda_3 t_1+\lambda_2\lambda_4 t_2+m^2(\lambda_1\lambda_2+\lambda_3\lambda_4)-m^2C(\lambda)^2, \tag{17b}$$

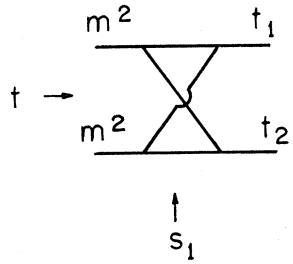

FIG. 7. Diagram for the amplitude $\bar{A}_1$. When g_i and β_1 are included, we obtain A_1.

$$C(\lambda)=\lambda_1+\lambda_2+\lambda_3+\lambda_4, \tag{17c}$$

$$s_1+t+u_1=2m^2+t_1+t_2. \tag{17d}$$

This can be written in the more familiar Feynman representation as

$$A_1(s_1,t;t_1,t_2)\propto\int_0^1\left(\prod_{i=1}^{4}d\alpha_i\right)\delta(1-C)\times\left(\frac{\alpha_2+\alpha_4}{C(\alpha)}\right)^{\phi_1}\left(\frac{\alpha_1+\alpha_3}{C(\alpha)}\right)^{\phi_2}\frac{1}{[D(\alpha,s_1,u_1)]^2}. \tag{17e}$$

Note that for $\phi_1=\phi_2=0$, A_1 reduces to $\bar{A}_1$, the ordinary Feynman amplitude of Fig. 7.

From Eq. (17e) the analytic properties of A_1 can be read instantly. First, A_1 has the same Landau curves as $\bar{A}_1$ because these come from $D(\alpha,s_1,u_1)$. Second, the term $\beta_1^{\phi_1}$ does not introduce a new singularity because if $\alpha_2=\alpha_4=0$, then

$$D(\alpha,s_1,u_1)=\alpha_1\alpha_3 t_1-(\alpha_1+\alpha_3)^2m^2;$$

but since $t_1<0$, then D is strictly negative and cannot pinch with $\beta_1^{\phi_1}$. Finally, it can be seen from Eq. (17b) that for

$$s_1,u_1<2m^2$$

D is strictly negative; therefore, A_1 is strictly real there. This region, labeled D_2, is shown in Fig. 8. We summarize the results in Fig. 9(a). The expression for A_1 in Eq. (17e) in terms of invariants also allows us to write

$$A(s,t)\propto\int\frac{dt_1dt_2}{(-\lambda)^{1/2}}\times\left(\frac{s}{i}\right)^{\phi_1(t_1)+\phi_2(t_2)-1}N_1(t,t_1,t_2)N_2(t,t_1,t_2), \tag{18a}$$

$$N_i(t,t_1,t_2)=\int_{-\infty}^{+\infty}ds_i A_i(s_i,t;t_1,t_2). \tag{18b}$$

We can now bring $A(s,t)$ to the form of the absorption model. In Fig. 9(a) we distort the contour of integration around the right-hand cut. [$A_1\to(\ln s_1)/s_1^2$ as $s_1\to\infty$.]

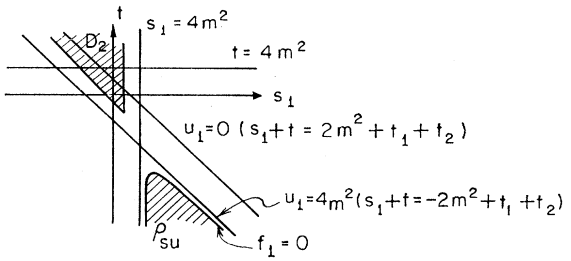

FIG. 8. Analytic properties of A_1; A_1 has singularities at $s_1=4m^2$, $u_1=4m^2$, and $f_1=0$ (boundary of double spectral function), and it is real in D_2.

[20] I. T. Drummond, P. V. Landshoff, and W. J. Zakrzewski, Nucl. Phys. **B11**, 383 (1969).

[21] P. V. Landshoff and J. C. Polkinghorne, Phys. Rev. **181**, 1989 (1969).

[22] We are very indebted to P. V. Landshoff for suggesting this approach.

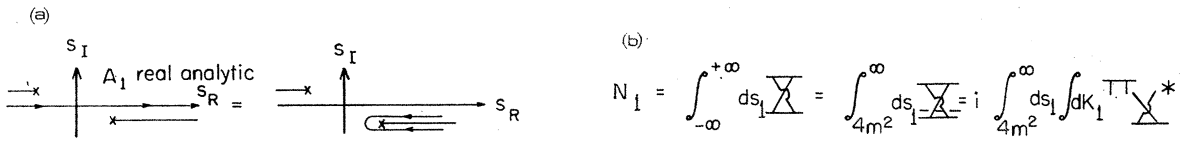

FIG. 9. (a) Contour of integration for N_1. (b) Representation for N_1 of Fig. 4 in terms of the integral of the absorptive part of A_1.

Then

$$N_1(t,t_1,t_2) \propto \int_{4m^2}^{\infty} ds_1 \,\mathrm{disc}[A_1(s_1,t;t_1,t_2)]. \quad (19a)$$

Since A_1 is real analytic between the cuts of Fig. 9(a), note that

$$\mathrm{disc}[A_1]=2i\,\mathrm{Im}A_1\,. \quad (19b)$$

Since the discontinuity is generated by the denominators d_2, d_3, and since A_1 is real analytic, we can invoke a Cutkosky-type theorem to give

$$N_1(t,t_1,t_2) \propto i\int_{4m^2}^{\infty} ds_1 \times \int \frac{d\alpha_1 d\beta_1 dK_1}{d_1 d_4} \beta_1^{\phi_1}(1-\beta_1)^{\phi_2}\delta(d_2)\delta(d_3)F\,, \quad (19c)$$

where F involves the Jacobian of the transformation to mass variables. Integrating on the δ functions, we obtain

$$N_1(t,t_1,t_2) \propto i\int_{4m^2}^{\infty} ds_1 \int dK_1 B^U B^{L*}\,, \quad (19d)$$

where

$$B^U = \frac{\beta_1^{\phi_1}}{d_1}(F)^{1/2}\Big|_{d_2=d_3=0}\,, \quad B^L = \frac{(1-\beta_1)^{\phi_2}}{d_4}(F)^{1/2}\Big|_{d_2=d_3=0}\,. \quad (19e)$$

In terms of graphs, we can write N_1 as in Fig. 9(b).

Thus we can split N_1 into an integral of factors $B^U B^{L*}$, where B^U involves the upper part of the diagram and B^L involves the lower part. Performing the same operation on N_2, we get

$$N_2 \propto i\int_{4m^2}^{\infty} ds_2 \int dK_2 C^U C^{L*}. \quad (19f)$$

Returning to Eq. (18a), we can bring $A(s,t)$ to the form

$$A(s,t) \propto \frac{-i}{s}\int \frac{dt_1 dt_2}{(-\lambda)^{1/2}} dK_1 dK_2 \times\left[B^U\left(\frac{s}{-i}\right)^{\phi_1(t_1)} C^U\right]\left[B^{L*}\left(\frac{s}{-i}\right)^{\phi_2(t_2)} C^{L*}\right]. \quad (20a)$$

Writing

$$M_1 = B^U(s/i)^{\phi_1}C^U\,, \quad M_2 = B^L(s/i)^{\phi_2}C^L\,, \quad (20b)$$

we finally arrive (see Fig. 10) at

$$A(s,t) \propto \frac{-i}{s}\int dK dK_1 dK_2 M_1 M_2^* e^{-i\pi\phi_2(t_2)}. \quad (20c)$$

With B and C real, Eq. (20a) agrees with the absorption model. In particular, when ϕ_1 is the Pomeranchuk pole, then $A(s,t)$ interfers destructively with the pole term of ϕ_2. In Eq. (20c) the extra phase term restores the correct phase to the M_2 amplitude.

To extend this result and prepare for the general diagram of Sec. II D, we briefly discuss the diagram of Fig. 11. There are several noteworthy features.

In the first place, one sees that on the left-hand side of the diagram only the lines 1, 3, 5, and 7 attach to Regge amplitudes. Hence we might suspect that only these are subject to the finite-mass condition. It turns out this would not give enough conditions to provide an immediate solution for the Sudakov variables. There are two ways we can argue to extend the class 1,3,5,7: On the one hand, we can argue that, in the spirit of Arnold,[10] HKPR,[5] and of the work to follow in Sec. III, the external physical particles should themselves also be Reggeized. This would place form factors on the external vertices also, and would lead to the requirement that the lines 2 and 6 also satisfy the finite-mass condition, and would provide enough lines to perform the Gribov analysis. On the other hand, Polkinghorne[23] has recently extended the Gribov analysis to diagrams with internal Reggeons constructed from Veneziano amplitudes without any form factors at all. The integrations are done by a steepest-descent analysis, and, as it turns out, this leads to the desired finite-mass conditions on all internal lines (see also Refs. 24 and 25).

In any event, after satisfying the finite-mass conditions, one finds, in the same way as before,

$$\alpha_1,\alpha_2,\alpha,\beta,\beta_3,\beta_4 \sim \Lambda/s\,, \quad 0<\beta_1,\beta_2,\alpha_3,\alpha_4<1\,.$$

One again obtains the amplitude $A(s,t)$ in the same form

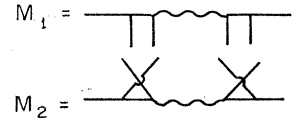

FIG. 10. Single scattering amplitudes M_1, M_2 of Eq. (20c).

[23] J. C. Polkinghorne, Phys. Rev. **186**, 1670 (1969). See also Refs. 24 and 25.
[24] S. N. Negrine, Nuovo Cimento **68A**, 165 (1970).
[25] G. A. Winbow, Phys. Rev. **177**, 2533 (1969).

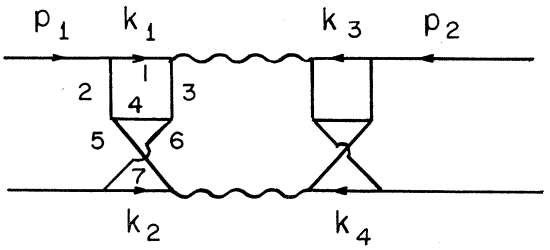

FIG. 11. Extension of the Mandelstam diagram.

as before, with the amplitude $A_1(s_1,t;t_1,t_2)$ now given by

$$A(s_1,t;t_1,t_2)=\int_0^1 d\beta_1 d\beta_2 \beta_1^{\phi_1}\beta_2^{\phi_2} g_1 g_2 \times\int_{-\infty}^{+\infty} d\alpha_1 d\alpha_2 dK_1 dK_2 / \prod_{i=1}^{7} d_i. \quad (21)$$

The amplitude $N_1(t,t_1,t_2)$ is given by a sum of four unitarity terms (Fig. 12). Therefore, $A(s,t)$ takes the form

$$A(s,t)\propto\sum_{i,j}\frac{-i}{s}\int d\Omega_i \times\left[B_i^U\left(\frac{s}{-i}\right)^{\phi_1}C_j^U\right]\left[B_i^{L*}\left(\frac{s}{-i}\right)^{\phi_2}C_j^{L*}\right], \quad (22)$$

a sum of all possible unitarity cuts on the left-hand side of the diagram times all possible cuts on the right.

C. Diagrams without Cuts

We now pass on to diagrams that do not have cuts. The essential point we shall demonstrate is that a diagram has a cut if it has third double-spectral functions on its sides. As we shall see in Sec. III, this will tie in conveniently with our physical ideas about the composite structure of physical particles.

To demonstrate this relation we will show that the amplitude of any diagram with two-Reggeon exchange (Fig. 13) can be brought to the form

$$A(s,t)\propto\int dK\left(\frac{s}{-i}\right)^{\phi_1+\phi_2-1} N_1 N_2, \quad (23a)$$

where N_i is related[26] to the amplitude of the blobs

$$N_1(t,t_1,t_2)\sim\int_{-\infty}^{+\infty} ds_1 A_1(s_1,t;t_1,t_2). \quad (23b)$$

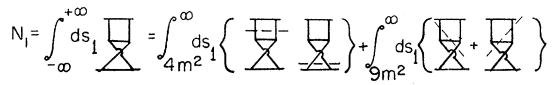

FIG. 12. Representation for N_1 of Fig. 11 in terms of the integral of the absorptive parts of A_1.

[26] J. C. Polkinghorne, Nucl. Phys. **B6**, 441 (1968).

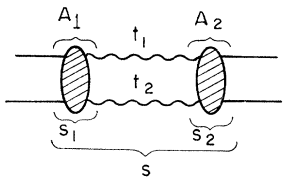

FIG. 13. General two-Reggeon-exchange diagram.

Furthermore, if A_1 has a third double-spectral function, then the integral in Eq. (23b) is nonzero. But if A_1 has no third double-spectral function, then N_1 is identically zero; in this case, Eq. (23a) is also zero and the leading behavior of $A(s,t)$ is of lower order in s than Eq. (23a).

We saw earlier that the leading behavior of the AFS diagram vanishes as $s\to\infty$. [It behaves as $(\ln s)/s^3$.] Its amplitude can be brought to the form of Eq. (23a) even though the coefficients N_1, N_2 are zero. To do this, apply the Gribov analysis to Fig. 3:

$$\begin{aligned} d_1&=(p_1-k)^2=(1-\beta)(m^2/s-\alpha)s+K^2-m^2+i\epsilon\,,\\ d_2&=(p_2+k)^2=(1+\alpha)(m^2/s+\beta)s+K^2-m^2+i\epsilon\,. \end{aligned} \quad (23c)$$

Then $d_1,d_2\sim O(\Lambda)$ gives $\alpha\sim\beta\sim O(\Lambda/s)$; setting $\alpha\to\alpha s$, $\beta\to\beta s$, we have

$$d_1=-\alpha+K^2+i\epsilon,\quad d_2=\beta+K^2-i\epsilon,\quad t_1=K^2,\quad t_2=(K-Q)^2.$$

Since we have kept d_1,d_2 finite as s went to infinity, we can write the Regge amplitudes in factorized form,

$$R=g_1(d_1,t_1)\left(\frac{s}{-i}\right)^{\phi_1(t_1)} g_2(d_2,t_2)\,,$$

$$R'=g_1'(d_1,t_1)\left(\frac{s}{-i}\right)^{\phi_2(t_2)} g_2'(d_2,t_2)\,.$$

The amplitude takes the form of Eq. (23a) with

$$N_1(t,t_1,t_2)=\int_{-\infty}^{+\infty} d\alpha\frac{g_1}{d_1}g_1'=\int_{-\infty}^{+\infty} ds_1 A_1(s_1,t;t_1,t_2). \quad (24)$$

In Eq. (24) the integrand as a function of α has pole and cut singularities in the lower half-plane (Fig. 14). Since the form factors decrease as $d_1\to\infty$,

$$g_1(d_1,t_1)\to 0 \quad \text{as} \quad d_1\to\infty\,,$$

we can close the α contour of integration in the upper half-plane and get for N_1 zero, as expected. We conclude that Eq. (23) holds for the AFS amplitude, but its value is zero.

In the discussion of the AFS diagram, we need to invoke properties of the form factors in order to prove

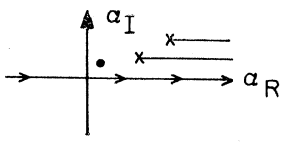

FIG. 14. Contour of integration in α for N_1 of Fig. 3.

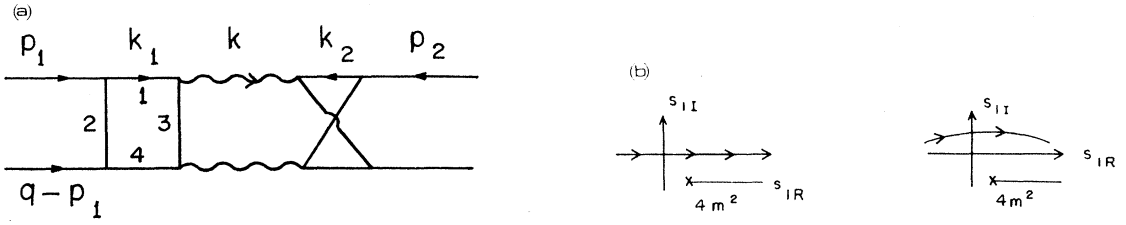

FIG. 15. (a) Diagram without a cut. (b) Contour of integration in s_1 for N_1 of Fig. 15(a).

that the amplitude does not persist. For the diagram of Fig. 15(a), we must also employ knowledge of the form factors. However, for more complicated diagrams (Fig. 20, for example), the absence of the cut rests completely on the absence of the third double-spectral functions.

Consider Fig. 15(a). After performing the finite-mass analysis, we arrive at Eq. (23) with

$$A_1=\int_0^1 d\beta_1\int_{-\infty}^{+\infty}\frac{d\alpha_1 dK_1}{d_1d_2d_3d_4}\times\beta_1{}^{\phi_1+\phi_2}g_1(d_1,d_3,t_1)g_1'(d_3,d_4,t_2)\,. \quad (25a)$$

As a function of s_1, A_1 has only a right-hand cut in the lower half-plane, so in Eq. (23b) we are tempted to close the s_1 contour of integration in the upper half-plane [Fig. 15(b)]. This cannot be done if we ignore the form factors because the amplitude without form factors satisfies

$$\bar{A}_1(s_1,t;\,t_1,t_2)\longrightarrow(\ln s_1)/s_1\,. \quad (25b)$$

Therefore, the contour cannot necessarily be closed. We must invoke the presence of the form factors. We do this by interchanging the orders of integration in Eq. (23b) and first integrating on α ($\sim -s_1$). Then

$$N_1=\int\frac{d\beta_1 d\alpha_1 dK_1}{d_1d_2d_4}\beta_1{}^{\phi_1+\phi_2}\int_{-\infty}^{+\infty}\frac{d\alpha\; g_1g_2}{d_3}\,. \quad (25c)$$

The α integrand has singularities in α in the upper half-plane. The contour can be closed in the lower half-plane. Since g_1 and g_2 decrease as d_3 becomes large, we see that the α integral is zero. The remaining integrals in Eq. (25c) converge, and hence $N_1=0$.

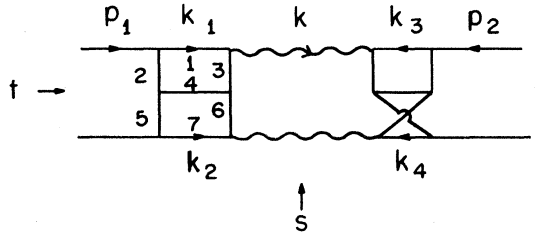

FIG. 16. Diagram without a cut.

Finally, we discuss the diagram of Fig. 16, which will lead to the general case of Sec. II D. We obtain Eq. (38), with

$$A_1=\int(d\alpha_1 d\beta_1 dK_1 d\alpha_2 d\beta_2 dK_2/\prod_{i=1}^{7}d_i)\beta_1{}^{\phi_1}\beta_2{}^{\phi_2}g_1g_1'\,. \quad (26)$$

Again, A_1 has only a right cut, but now the amplitude without form factors satisfies

$$\bar{A}_1\longrightarrow(\ln s_1)/s_1{}^2\quad\text{as}\quad s_1\longrightarrow\infty\,,$$

and hence the contour of integration in Eq. (23b) can be closed in the upper half-plane to give $N_1=0$. For Fig. 16 the absence of the cut is thrown entirely on the absence of the third double-spectral function.

D. General Case

We now come to a general class of two-Reggeon-exchange diagrams which is the basis for our derivation of the absorption model. Just how general can this class be? What we are interested in is the amplitude for a diagram of the type of Fig. 13. However, we do not wish the amplitudes A_i to be completely arbitrary, because in the form of the absorption model we are interested in we require that they be strictly low-energy amplitudes relative to s. That is, we require that the incident energy s flow across the Reggeons and not down the sides of the diagram, because we will want to identify the A_i with direct-channel physical particles near the mass shell.

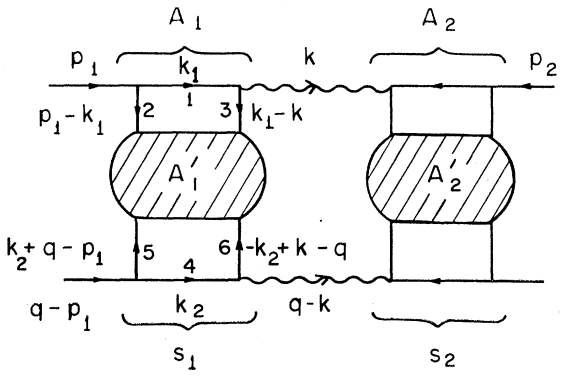

FIG. 17. General two-Reggeon-exchange diagram with low-energy direct-channel amplitudes.

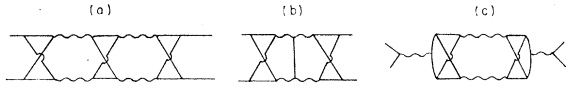

FIG. 18. Diagrams not contained in Fig. 17.

Note that the diagrams we have studied satisfy this condition. For example, we have found that whereas the four-momenta on the sides of the diagrams can become large (e.g., $k_1=\beta_1 p_1'+\alpha_1 p_2'+K_1$, $0<\beta_1<1$, $\alpha_1\sim\Lambda/s$), the energies s_i always remain finite relative to s (e.g., $s_1=-\alpha s+m^2+K^2$, $\alpha\sim\Lambda/s$). The large energy s flows only across the Reggeons.

It is not hard to convince oneself that a general type of diagram satisfying these conditions is that of Fig. 17 below. The effect of the elementary lines 1,2 is to tell us where the internal Reggeon line ends and to prevent A_1 from having Regge behavior in s. Thus Fig. 17 excludes all the diagrams of Fig. 18. It includes all the diagrams discussed before. (For the double crossed diagram, A_1' in Fig. 17 would be various δ functions.) It also includes the diagram of Fig. 19, if the lines n_i are grouped into a single line of mass M. Most important, it includes the diagram of Fig. 20(a). When the rungs in the direct channel are summed over, this provides a model for the Regge box diagram of Fig. 20(b) (first introduced by Arnold and discussed in HKPR).

We consider, then, the diagram of Fig. 17. We use the notation

$$A=A(s,t)\,,\quad A_1=A_1(s_1,t;t_1,t_2)\,,\quad A_1'=A_1(s_1,t_1',u_1';d_i)\,.$$

The amplitude A_1' is to be quite general; we are interested only in whether or not it has a third double-spectral function, and so write it in the form

$$A_1'=\int_{4m^2}^{\infty}d\zeta\,\frac{f(s_1,\zeta)}{\zeta-t_1'}+\int_{4m^2}^{\infty}d\zeta\,\frac{g(s_1,\zeta)}{\zeta-u_1'}\,; \tag{27a}$$

that is, we can treat A_1' as a propagator of mass $\zeta\geq 4m^2$. The analysis now goes through as before. We indicate the essential features.

After the finite-mass analysis has been performed, $A(s,t)$ takes the expected form of Eq. (23a) and (23b) with

$$A_1(s_1,t;t_1,t_2)=\int_0^1 d\beta_1 d\beta_2$$

$$\times\int_{-\infty}^{+\infty}(d\alpha_1 d\alpha_2 dK_1 dK_2/\prod_{i=1}^{5}d_i)\beta_1^{\phi_1}\beta_2^{\phi_2}g_1 g_2 A_1'\,, \tag{27b}$$

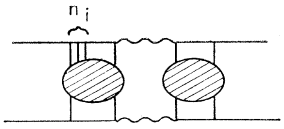

FIG. 19. Class of diagrams contained in Fig. 17.

where

$$\begin{aligned}
&d_1=\alpha_1\beta_1+K_1^2-m^2+i\epsilon\,,\\
&d_2=(\alpha_1-m^2)(\beta_1-1)+K_1^2-m^2+i\epsilon\,,\\
&d_3=(\alpha_1-\alpha)\beta_1+(K_1-K)^2-m^2+i\epsilon\,,\\
&d_4=\alpha_2\beta_2+K_2^2-m^2+i\epsilon\,,\\
&d_5=(\alpha_2+t-m^2)(\beta_2-1)+(Q+K_2)^2-m^2+i\epsilon\,,\\
&d_6=(\alpha_2+t-\alpha)\beta_2+(K_2+Q-K)^2-m^2+i\epsilon\,,\\
&s_1=-\alpha+K^2+m^2\,,\quad u_1=m^2+\alpha-t+(K-Q)^2\,,\\
&t_1'=(\alpha_2+t-\alpha_1)(\beta_2-\beta_1)+(K_2+Q-K_1)^2\,,\\
&u_1'=(\alpha_1+\alpha_2+t-\alpha-m^2)(\beta_1+\beta_2-1)\\
&\qquad\qquad+(K_1+K_2+Q-K)^2\,.
\end{aligned} \tag{28}$$

We consider separately the cases of the t_1' and u_1' dispersion contributions.

u_1' Contribution

As before, the first task is to establish the analytic properties of the amplitude A_1. This can again be done by introducing Feynman parameters. The amplitude A_1 takes the form

$$A_1(s,u_1;t_1,t_2)=\int_{4m^2}^{\infty}d\zeta\,f(s_1,\zeta)F_1(s_1,u_1;t_1,t_2,\zeta)\,, \tag{29a}$$

$$F_1=\int_0^{\infty}d\lambda_1\cdots d\lambda_7$$

$$\times[\beta_1(\lambda)]^{\phi_1}[\beta_2(\lambda)]^{\phi_2}\frac{e^{iD(\lambda,s_1,u_1,\zeta)/C(\lambda)}}{[C(\lambda)]^2}\,, \tag{29b}$$

$$\propto\int_0^1 d\alpha_1\cdots d\alpha_7\delta(1-\Sigma\alpha_i)$$

$$\times\frac{C(\alpha)}{[D(\alpha,s_1,u_1,\zeta)]^3}[\beta_1(\alpha)]^{\phi_1}[\beta_2(\alpha)]^{\phi_2}\,, \tag{29c}$$

where

$$\beta_1(\alpha)=[\alpha_2(\alpha_4+\alpha_5+\alpha_6+\alpha_7)+\alpha_7(\alpha_4+\alpha_6)]/C(\alpha)\,, \tag{29d}$$

$$\beta_2(\alpha)=[\alpha_5(\alpha_1+\alpha_2+\alpha_3+\alpha_7)+\alpha_7(\alpha_1+\alpha_3)]/C(\alpha)\,, \tag{29e}$$

$$C(\alpha)=\sum_1^7\alpha_i\,, \tag{29f}$$

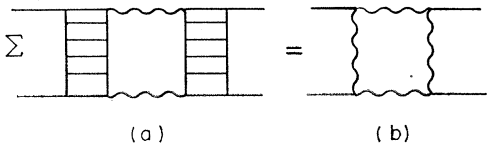

FIG. 20. Representation of the Regge box diagram in terms of diagrams of the class of Fig. 17.

$$D=s_1[\alpha_2\alpha_3(\alpha_4+\alpha_5+\alpha_6+\alpha_7)+\alpha_5\alpha_6(\alpha_1+\alpha_2+\alpha_3+\alpha_7)$$
$$+\alpha_2\alpha_5\alpha_7+\alpha_3\alpha_6\alpha_7]+u_1\alpha_1\alpha_4\alpha_7$$
$$+m^2[\alpha_1\alpha_2(\alpha_4+\alpha_5+\alpha_6+\alpha_7)+\alpha_1\alpha_6\alpha_7]$$
$$+m^2[\alpha_4\alpha_5(\alpha_1+\alpha_2+\alpha_3+\alpha_7)+\alpha_3\alpha_4\alpha_7]$$
$$+K^2[\alpha_1\alpha_3(\alpha_4+\alpha_5+\alpha_6+\alpha_7)+\alpha_1\alpha_5\alpha_7]$$
$$+(Q-K)^2[\alpha_4\alpha_6(\alpha_1+\alpha_2+\alpha_3+\alpha_7)+\alpha_3\alpha_4\alpha_7]$$
$$-[\alpha_7\zeta+(\sum_{i=1}^{6}\alpha_i)m^2][(\alpha_1+\alpha_2+\alpha_3)(\alpha_4+\alpha_5+\alpha_6)$$
$$+\alpha_7(\alpha_1+\alpha_2+\alpha_3+\alpha_4+\alpha_5+\alpha_6)]. \quad (29g)$$

The analytic properties of A_1 now follow easily. First, A_1 has all the singularities that $\bar{A}_1$ has because they are determined by the Feynman discriminant D of Eq. (29g). Second, A_1 does not have any new singularity arising from the β_i factors. If β_1 vanishes, say, then various α_j in Eq. (29d) also vanish. Further, since we have assumed $\phi_1>-1$, $\beta_1^{\phi_1}$ is integrable; therefore, we are only interested in those singularities in which the propagators $d_1, \ldots, d_6$ also participate. This means that all the remaining α_j's must either vanish or pinch. However, these are just the conditions for a Landau singularity of the Feynman amplitude $\bar{A}_1$. We conclude that any singularity of A_1 associated with the vanishing of β_1 must already be a singularity of $\bar{A}_1$. Since the sheet structure of the singularities is determined by the $i\epsilon$ prescription in D and is unaffected by the presence of the $\beta_1^{\phi_1}$, we see that A_1 has no more singularities than $\bar{A}_1$.

Third, it is easily seen from Eq. (29g) that D is strictly negative for $s_1,u_1<2m^2$; hence, A_1 is real in this region.

So we conclude that A_1 has the same real analytic properties as $\bar{A}_1$.

Now we can return to N_1 and bring it to the unitarity form. Since A_1 has left- and right-hand thresholds (Fig. 9), we can close the contour of integration around the right-hand cut to obtain (see Fig. 21)

$$N_1=\sum_i \int_{\Delta_i}^{\infty} ds_1 \,\mathrm{disc}[A_1]=2i\sum_i \int_{\Delta_i}^{\infty} ds_1 B_i^U B_i^{L*}. \quad (30)$$

The sums in Eq. (30) are over all possible s_1-channel unitarity cuts with thresholds Δ_j.

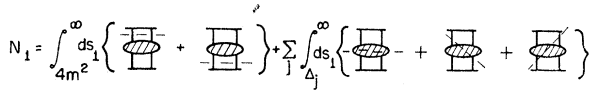

FIG. 21. Representation of N_1 of Fig. 17 in terms of absorptive parts of A_1.

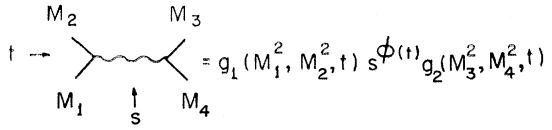

FIG. 22. Regge amplitude with form factors representing composite external particles.

The amplitude A becomes

$$A(s,t)=-2i\sum_{i,j}\int dK ds_1 ds_2$$
$$\times\left[B_i^U\left(\frac{s}{i}\right)^{\phi_1}C_i^U\right]\left[B_i^{L*}\left(\frac{s}{i}\right)^{\phi_2}C_i^{L*}\right]. \quad (31)$$

t_1' Contribution

The calculations proceed as before. One again verifies that A_1 has the same real analytic structure as $\bar{A}_1$. When we come to consider N_1, we observe that as a function of s_1 the integrand of Eq. (23b) has singularities that all lie in the lower half-plane. (This is another way of saying that A_1' has no left-hand cut.) Hence we can close the s_1 contour of integration in the upper half-plane to get zero. Therefore $N_1\equiv 0$, and $A(s,t)$ does not persist.

III. PHYSICAL IMPLICATIONS—COMPOSITENESS, MULTIPLE SCATTERING, AND ABSORPTION MODEL

Now consider the relationship between the mathematical results obtained and the physical meaning of compositeness and multiple scattering. It is not hard to see why the AFS diagram does not give the double scattering we would expect. On the one hand, the form of a Reggeon amplitude in Fig. 22 implies a compositeness of the external particles M_i which is reflected in the form factor dependence on M_i. It was through just this dependence that the Rothe cancellation occurred. This compositeness is also reflected through the ladder representation of a Reggeon (Fig. 23). On the other hand, when the Reggeon of Fig. 22 is inserted in an AFS diagram, the external particles M_1,M_4 are given elementary particle propagators. We claim it is this inconsistency that deprives the AFS diagram of a cut.

What must be done is either to remove the M_i dependence from Fig. 22 or to represent the external particles M_i by more realistic propagators. We would like to discuss the second alternative.

It is our belief, in the spirit of Arnold, HKPR, and Yang, that physical particles are complicated composite objects. In a Bethe-Salpeter framework, for example,

FIG. 23. Ladder representation of a Reggeon. 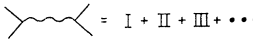

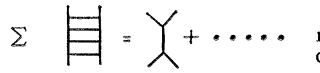

FIG. 24. Bethe-Salpeter representation of composite physical particles.

one writes the equation of Fig. 24, where the right-hand side represents the physical pole of the left-hand side.

In a scattering process of a physical particle, some of the constituent pieces of matter take part in the scattering, while the rest stands by as a spectator not taking part. A single-scattering process that is drawn as Fig. 25(a) microscopically looks like Fig. 25(b), where the double lines are the physical particles and the single lines are their constituents. Similarly, a double-scattering process that is drawn as Fig. 26(b) should actually be drawn as Fig. 25(b). The incident particle at 1 separates into scattering and spectator constituents. At 2 the constituents unite to form a physical particle in the intermediate state. At 3 the same process occurs again, and the physical particle emerges at 4.

In a field-theory model, the intermediate physical particle can be represented by the direct-channel ladders of Fig. 23. We can interpret this as a direct-channel Reggeon. This suggests Fig. 27(a). From the results of Sec. II D, we know that Fig. 27(a) does not have a cut because the sides lack third double-spectral functions. Physically, this corresponds to an apparent cancellation between the contributions to $\int ds_1 \times A_1(s_1,t;t_1,t_2)$ that come from even- and odd-signature physical particles in an exchange-degenerate trajectory. A direct-channel Reggeon with signature is represented as in Fig. 27(b). Figure 27(a) becomes replaced by Fig. 27(c), which has a cut.

In a phenomenological calculation, we replace the direct-channel amplitudes of Fig. 27(c) by the known physical particles. Thus, for $\pi^- p \to \pi^0 n$, the contribution

$$\int_{4m^2}^{\infty} ds_2 \,\mathrm{disc} A_2(s_2,t;t_1,t_2)$$

is written as in Fig. 28, where we include all recurrences of the p and continuum states. A typical term contributes

$$\int ds_1 \,\mathrm{disc}\left(\frac{g_{\rho pn} g_{ppP}}{s_2{}^2 - mp^2 + i\epsilon}\right) \propto i g_{\rho pn} g_{ppP}.$$

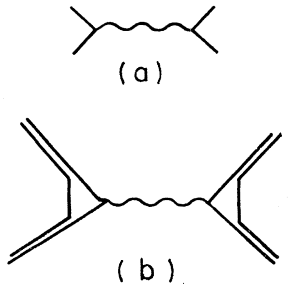

FIG. 25. Single scattering of composite systems.

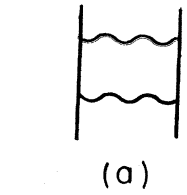

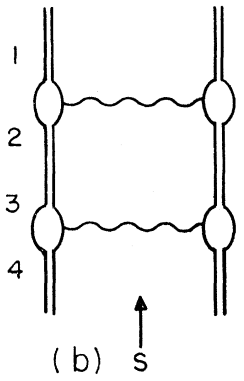

FIG. 26. Double scattering of composite systems.

The scattering amplitude becomes

$$A(s,t) \propto \frac{-i}{s}\int dK\, g_{\pi\pi\rho}\left(\frac{s}{-i}\right)^{\phi_1} g_{npp} g_{\pi\pi P}\left(\frac{s}{-i}\right)^{\phi_2} g_{ppP} \quad (32a)$$

$$\propto \frac{-i}{s}\int \frac{dt_1 dt_2}{(-\lambda)^{1/2}} M_\rho(s,t_1) M_{e1}(s,t_2). \quad (32b)$$

This is the absorption model.

In HKPR the contributions of the remaining terms of Fig. 28 are assumed to have the same s,t dependence as Eq. (32b), and are added by multiplying Eq. (32b)

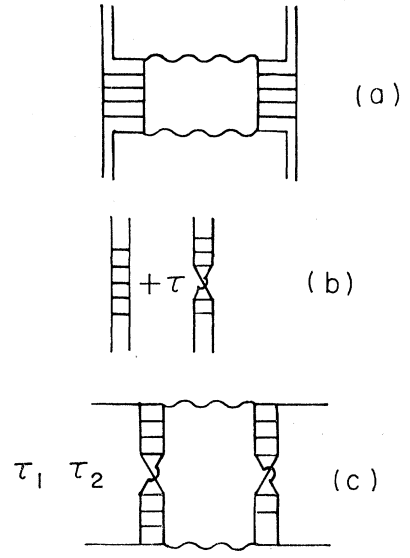

FIG. 27. (a) Two-Reggeon exchange with direct-channel ladders. (b) Ladder representation of a direct-channel Reggeon with signature. (c) Diagram for two-Reggeon exchange with direct-channel Reggeons with signature.

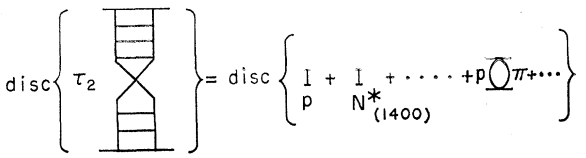

FIG. 28. Contributions to the amplitude N_2 from the direct-channel physical states that are contained in A_1.

by a factor λ. It has been shown[27] that the amplitude for

$$p+p \to p+\text{anything} \tag{33a}$$

proceeding via Pomeranchuk exchange may be as large as 50% of the elastic amplitude

$$p+p \to p+p\,. \tag{33b}$$

This suggests that λ could be about 2.

IV. COMPARISON WITH WORK OF GRIBOV *et al.*

In Ref. 28, Gribov and Migdal studied amplitudes generated by the exchange of a Regge pole. Their program is to write a Reggeon field theory that can be solved by summing Reggeon diagrams to determine the scattering amplitude. For example, the amplitude involving the Pomeranchuk cut and the PP cut is given by Fig. 29. This implies for the absorption model that in addition to the diagrams of Fig. 2 one must consider effects of t-channel iteractions in Fig. 30. It is well known that if the diagrams of Fig. 30(c) are summed, the sum has a pole term related to the pole of Fig. 29(a), and a cut term related to the cut of Fig. 29(b). Is one double counting by including the pole of Fig. 29(a) separately? Compelling physical arguments have been given in HKPR for why this is not so, and why the physics of elastic absorption is different from the physics of quantum-number exchange.

Gribov and collaborators[28,29] derived the absorption model from diagrams. We compare their derivation with ours. For their discussion of N_1, they write the equation of Fig. 31. They argue in a general fashion that A_1 has no new singularities or complexity from the presence of the $\beta_i^{\phi i}$. Therefore the discontinuity of A_1 can be calculated as for ordinary amplitudes by cutting the diagram and replacing the lower amplitude by its complex conjugate. They also give a proof for elastic scattering that $\lambda>1$. Our approach differs from theirs in that we have attempted to present a specific model for the two-Reggeon diagram that is based on our

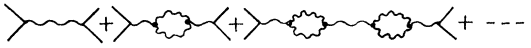

FIG. 29. Graphs in the Reggeon perturbation theory of Gribov and Migdal.

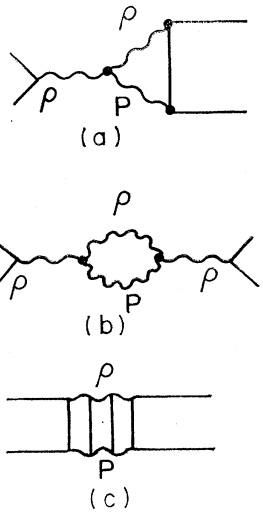

FIG. 30. Graphs that have not been included in the derivation of the absorption model. These graphs have amplitudes A_i that have large subenergies.

physical understanding of compositeness and multiple scattering, and to derive the absorption formula from that model.

Kaidalov and Karnakov[29] have considered the effect of the form factors on the convergence of the s_1 integral for N_1 at infinity.

Ter-Martirosyan[30] has derived the two-Reggeon cut from the AFS diagram by using form factors for the internal Reggeons that are evaluated on the mass shell. The Rothe cancellation mechanism is removed, and the contribution from the "elementary" propagators evaluated near the mass shell gives the expected form of the cut.

He also considers higher-order cuts (Fig. 32) and derives the eikonal formula of Arnold. How do his results affect ours? In a phenomenological absorption model, one needs to consider only the ρP cut. All elastic multiple scatterings are grouped into a single P term which is parametrized and fit by experiment [Fig. 33(a) and 33(b)]. The $PP\rho$ cut [Fig. 33(c)] is found to be small. Any cut involving $P\rho$ and a non-Pomeranchon [Fig. 33(d)] is small because the branch point is well below the ρ pole.

V. ASSUMPTIONS, CONCLUSIONS, AND FUTURE AREAS OF WORK

Assumptions

(a) Physical particles are composite objects, and when regarded as Reggeons they have definite signature.

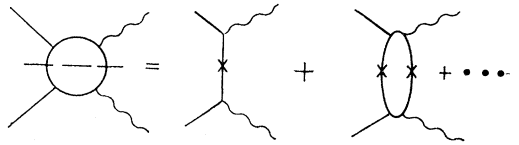

FIG. 31. Equation Gribov and Migdal use to relate N_1 to direct-channel physical states.

[27] J. Pumplin and M. Ross, Phys. Rev. Letters **21**, 1778 (1968).
[28] V. N. Gribov and A. A. Migdal, Yadern. Fiz. **8**, 1002, 1213 (1968) [Soviet J. Nucl. Phys. **8**, 583, 703 (1969)].
[29] A. B. Kaidalov and B. M. Karnakov, Phys. Letters **29B**, 372 (1969).
[30] K. A. ter-Martirosyan, Yadern. Fiz. **10**, 1047 (1969); **10**, 1262 (1969) [Soviet J. Nucl. Phys. **10**, 600 (1970); **10**, 715 (1970)].

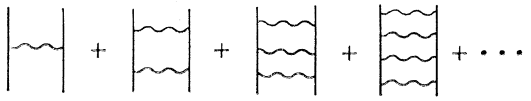

FIG. 32. s-channel iterations of the Pomeranchon that give the eikonal.

(b) Multiple scattering of composite systems can be treated in a Glauber scatterer-spectator approach. (c) The leading behavior of a Feynman amplitude is given by the Gribov finite-mass conditions; the second-order term is down by a factor of $1/s$ from the leading behavior.

Conclusions

The amplitude for the diagram of Fig. 13, where A_i are low-energy amplitudes relative to s, is given by the absorption formula

$$A(s,t) \propto +i\int dK\, s^{\phi_1+\phi_2-1}e^{\frac{1}{2}i\pi(\phi_1+\phi_2)}N_1N_2$$
$$\propto -i\int\frac{dK}{s}M_1(s,t_1)M_2(s,t_2)+\cdots .$$

Future Areas of Work

(a) What is the effect of t-channel iterations? (b) What is the relation between the absorption-model approach and the bootstrap approach? (See Ref. 31.) (c) Is $\lambda>1$?

ACKNOWLEDGMENTS

A part of the present work was done with the assistance of Dr. F. Henyey—in particular, the formulation of the finite-mass condition, the necessity of proving real analyticity of A_1, and a discussion of the work by HKPR. We wish to thank Professor Marc Ross for suggesting the present problem and for constant encouragement of its development through many stages over a long period of time. I am also grateful to Dr. G. Kane and Dr. R. Kelly for helpful suggestions.

The work could not have been undertaken without a sustained and fruitful interaction with the Cambridge group. I wish to thank Professor J. C. Polkinghorne, Professor R. J. Eden, Dr. I. T. Drummond, Dr. P. V. Landshoff, Dr. D. I. Olive, Dr. G. Winbow, and Dr. S. Negrine for long and instructive discussions. I am grateful to Professor G. Chew for the hospitality of the Lawrence Radiation Laboratory as an AEC Fellow.

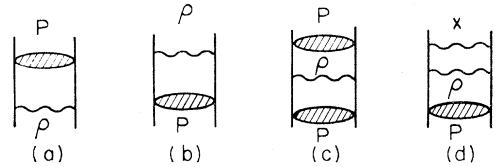

FIG. 33. Cuts generated by the ρ. Diagrams (a) and (b) are used in the absorption model; (c) and (d) have small contributions.

[31] L. Caneschi, Phys. Rev. Letters **23**, 254 (1969).

APPENDIX A: CUTS WITH VENEZIANO AMPLITUDES

An essential condition for the AFS diagram not to have a cut is the presence of the form factors. What happens when the Reggeons are represented as Veneziano amplitudes with no form factors? The amplitude of Fig. 3 becomes

$$A(s,t)=\int\frac{sd\alpha d\beta dK}{d_1d_2}R(s,t_1)R(s,t_2)\,, \tag{A1}$$

where d_1 and d_2 are given by Eq. (23c) and $t_1=\alpha\beta s+K^2$, $t_2=(\alpha+t/s)(\beta-t/s)s+(Q-K)^2$. There are now no form factors and hence no Gribov finite-mass condition, but the integral (A1) can be evaluated directly.[24,32,33] We obtain the dominant contribution to (A1) from the region of integration $O(m^2/s)\leq\beta<1$ by evaluating the pole in α at $d_1=0$,

$$\alpha=m^2/s+(m^2-K^2)/(1-\beta)s\,. \tag{A2}$$

The β integrations can be done to give

$$A(s,t)\propto\int dK\, s^{\phi(K^2)+\phi[(Q-K)^2]-1}[\ln s+iO(i)]. \tag{A3}$$

The first term in the brackets comes from $O(m^2/s)<\beta<\epsilon$ and corresponds to d_2 going off the mass shell (ϵ is a small finite number). The second term comes from $\beta\sim O(m^2/s)$ when d_2 is on the mass shell, and corresponds to the usual AFS cut term. The asymptotic behavior of (A3) is then

$$A(s,t)\to s^{j_c(t)}[1+iO(1/\ln s)]\,, \tag{A4}$$

where

$$j_c(t)=2\phi(\tfrac{1}{4}t)-1\,. \tag{A5}$$

APPENDIX B: ALTERNATIVE PROOF OF REAL ANALYTICITY FOR A_1

One can also investigate real analyticity of the A_1 amplitudes directly using Sudakov variables. Consider Eq. (11). We see that if $0<\beta_1<1$, we can evaluate the α_1 integration directly by closing the A_1 contour in the lower half-plane and picking up the residues from d_1,d_3. Writing $d_i(j)$ as the value of d_i at the pole of d_j, and writing $D_i(j)=\beta_1 d_i(j)$, we obtain

$$A_1(s_1,t;t_1,t_2)\propto\int\int dK\int_0^1 d\beta_1\frac{\beta_1^{\phi_1+1}(1-\beta_1)^{\phi_2}}{d_3(1)}$$
$$\times\left[\frac{1}{D_2(1)D_4(1)}-\frac{1}{D_2(3)D_4(3)}\right], \tag{B1}$$

[32] Veneziano amplitudes in vertex diagrams have been evaluated by I. S. Gerstein, Kurt Gottfried, and Kerson Huang, Phys. Rev. Letters **24**, 294 (1970).

[33] The same technique is used for the vertex diagram. Clifford Risk, Phys. Rev. D **2**, 387 (1970).

where

$$
\begin{aligned}
d_3(1) &= -\alpha\beta_1 + (K_1-K)^2 - K_1^2 , \\
D_2(1) &= -[m^2-\beta_1(1-\beta_1)(m^2+\alpha-t)] \\
&\quad +(1-\beta_1)K_1^2+\beta_1(K_1+Q-K)^2 , \\
D_2(3) &= -[m^2-\beta_1(1-\beta_1)(m^2-\alpha)]+\beta_1 K_1^2 \\
&\quad +(1-\beta_1)(K_1-K)^2 , \qquad \text{(B2)} \\
D_4(1) &= -[m^2-\beta_1(1-\beta_1)(m^2+\alpha-t)]+(1-\beta_1)K_1^2 \\
&\quad +\beta_1(K_1+Q-K)^2 , \\
D_4(3) &= -[m^2-\beta_1(1-\beta_1)(m^2-t)] \\
&\quad +\beta_1(K_1-K+Q)^2+(1-\beta_1)(K_1-K)^2 .
\end{aligned}
$$

We immediately see that at the end points of integration—$\beta_1=0$, 1—the terms $D_i(j)$ are strictly negative and cannot vanish. The term $d_3(1)$ can vanish, but its residue is zero [i.e., $d_3(1)$ is a factor of the terms in the brackets]. Hence we conclude that the terms $\beta_1^{\phi_1}$ and $(1-\beta_1)^{\phi_2}$ do not introduce any new singularities.

Finally, we observe that A_1 is certainly a real quantity when the $D_i(j)$'s are negative for all β_1 between 0 and 1. This occurs when the terms in brackets of Eq. (B2) are positive. Since the maximum value of $\beta_1(1-\beta_1)$ is $\frac{1}{4}$, this condition is satisfied for

$$4m^2 > m^2+\alpha-t , \quad m^2-\alpha , \quad m^2-t .$$

This is equivalent to the region

$$s_1 < 4m^2+K^2 , \quad -3m^2 < t < 0 , \quad s_1+t > -2m^2+K^2 ,$$

which overlaps with the region D_2 of Fig. 8.

This method can also be applied to the amplitude A_1 of Fig. 17, but it becomes very tedious. The Feynman parameter method is considerably easier.

PHYSICAL REVIEW D VOLUME 3, NUMBER 2 15 JANUARY 1971

Higher-Order Terms in the Current-Current Theory of Weak Interactions*

R. S. Willey and J. M. Tarter
Department of Physics, University of Pittsburgh, Pittsburgh, Pennsylvania 15123
(Received 22 April 1970)

We examine the consequences of the hypothesis that, for some range of energies, the second-order terms in the perturbation expansion of the Fermi theory are small but non-negligible corrections to the first-order terms, and responsible for reactions which violate first-order selection rules. We compute matrix elements through second order in the weak coupling constant G and introduce subtraction constants which are necessary to render the matrix elements finite to this order. From this point of view we consider a number of weak-interaction problems, including the experimental parameters of μ decay, the universality of the μ-decay coupling constant and the Fermi β-decay coupling constant, K_{l3} decays, and $\Delta S=\Delta Q$ and $\Delta S=2$ semileptonic decays.

I. INTRODUCTION

THE phenomenological vector and axial-vector current-current description of weak interactions gives a good account[1] of a large number of experimental data. Nevertheless, it has been realized for some time that the phenomenological current-current matrix elements cannot be exact, because they lead to cross sections for leptonic reactions which violate the unitarity limit at very high energy. This suggests that the phenomenological current-current matrix elements are the first-order terms in a perturbation expansion of the S matrix. If this perturbation expansion is derived from a current-current interaction Lagrangian, it is not renormalizable in the conventional perturbation-theoretic sense. Thus one cannot predict whether higher-order effects are large or small (there is no small dimensionless coupling constant). The approach of this paper is based on the empirical observation that the lowest-order current-current matrix elements do give a good account of a large number of experimental data, so the higher-order effects are small at the energies presently accessible experimentally. This observed weakness of higher-order effects may occur term by term in a perturbation expansion, or it may only come out of a summation of all orders or some other nonperturbative approach. In this paper we explore the consequences of the former possibility. We offer no solution to the fundamental problem of divergences in a nonrenormalizable theory. We compute matrix elements through second order in the weak coupling constant G and introduce subtraction constants which are necessary to render the matrix elements finite to this order. We parametrize divergent integrals by undetermined subtraction constants in subtracted dispersion relations. We are able to show that some of these subtraction constants are "universal" (i.e., appear in the same way in more than one process); some others we guess, on more or less plausible grounds, to be

* Supported in part by the U. S. Atomic Energy Commission under Contract No. AT-30-1-3829.

[1] See, for example, the detailed description in R. E. Marshak, Riazuddin, and C. P. Ryan, *Theory of Weak Interactions in Particle Physics* (Wiley-Interscience, New York, 1969).